DTU Library

Itinerant Ferromagnetism in Ultracold Fermi Gases

Heiselberg, Henning

[Link back to DTU Orbit](#)

Itinerant Ferromagnetism in ultracold Fermi gases

H. Heiselberg

Applied Research, DALO, Lautrupbjerg 1-5, DK-2750 Ballerup, Denmark

Itinerant ferromagnetism in cold Fermi gases with repulsive interactions is studied applying the Jastrow-Slater approximation generalized to finite polarization and temperature. For two components at zero temperature a second order transition is found at $ak_F \simeq 0.90$ compatible with QMC. Thermodynamic functions and observables such as the compressibility and spin susceptibility and the resulting fluctuations in number and spin are calculated. For trapped gases the resulting cloud radii and kinetic energies are calculated and compared to recent experiments. Spin polarized systems are recommended for effective separation of large ferromagnetic domains. Collective modes are predicted and tri-critical points are calculated for multi-component systems.

I. INTRODUCTION

Ultracold Fermi systems with strong attraction between atoms has led to important discoveries as universal physics and the BCS-BEC crossover. Recently strongly repulsive interactions has been studied and a transition to a ferromagnetic phase was observed in the experiments of Jo et al. [1]. Earlier Bourdel et al. [2] and Gupta et al. [3] also observed a transition when the interactions became strongly repulsive near Feshbach resonances. A phase transition from a paramagnetic (PM) to ferromagnetic (FM) phase was predicted long ago by Stoner [4] based on the Hartree-Foch mean field energy and has recently been confirmed by more elaborate calculations including fluctuations [5, 6] and by QMC [7–9]. The calculated transition points and order of the transition differ also from experiment [1]. The FM transition is disputed by Zhai [10] who claims that the experimental data is compatible with strongly correlated repulsive Fermi systems which would explain the inability to observe FM domains in Ref. [1].

It the purpose of this work to clarify the phase diagram of strongly repulsive Fermi atomic systems as well as to calculate thermodynamic functions and measurable observables in atomic traps that clearly can distinguish the FM and PM phases and determine the order of the transition and the universal functions. By extending the Jastrow-Slater model [11–13] to finite polarization and temperature, we calculate the free energy and find a second order FM transition in a repulsive Fermi gas. A number of thermodynamic functions as the spin susceptibility, compressibility, and observables as radii and kinetic energies can be compared to experiments, and others as fluctuations, collective oscillations and phase separation can be predicted.

As a start the dilute limit model of Stoner is extended to finite temperature and the polarization and order of the transition is determined and compared to second order calculations. Subsequently, the Jastrow-Slater approximation is described for the correlated manybody wave-function in the strongly interacting limit and extended to finite polarization and temperature. Detailed calculations of the free energy and a number of thermodynamic functions are given. In particular the spin-susceptibility and compressibility are used for calculating fluctuations in spin and total particle number in section III. In section IV finite traps are considered and the cloud radii and kinetic energies are calculated and compared to recent experiments [1]. Collective modes are discussed in section V. Multi-components systems are discussed in section VI and a new string of critical points is found and plotted in a multi-component phase diagram. Finally, a summary and outlook is given.

II. FERROMAGNETIC TRANSITION

The models for repulsive ultracold Fermi gases in Refs. [4–8] all predict a phase transition somewhere near the unitarity limit $ak_F \sim 1$ but the phase diagrams disagree quantitatively as well as qualitatively concerning the order and critical points.

For a reference model we start with a simple finite temperature extension of the Hartree-Fock approximation originally studied by Stoner [4], which is a dilute limit expansion to first order in the scattering length. Subsequently, we calculate the phase diagram in the JS approximation and compare to those in the dilute limit to first [4] and second [5, 6] order as well as QMC [7, 8].

A. Dilute approximations

A dilute ($k_F a \ll 1$) degenerate Fermi gas with atoms in spin states $\sigma = 1, .., \nu$ with densities $\rho_\sigma = k_{F,\sigma}^3/6\pi^2$ and Fermi energy $E_{F,\sigma} = k_B T_{F,\sigma} = \hbar^2 k_{F,\sigma}^2/2m$ has the free energy

$$f = \frac{3}{5}\sum_\sigma E_{F,\sigma}\rho_\sigma + \sum_{\sigma<\sigma'}\frac{4\pi a}{m}\rho_\sigma\rho_{\sigma'} + f_T . \qquad (1)$$

It consists of the kinetic energy, the interaction energy to lowest order in the scattering length a as in the Stoner model [4], and the thermal energy
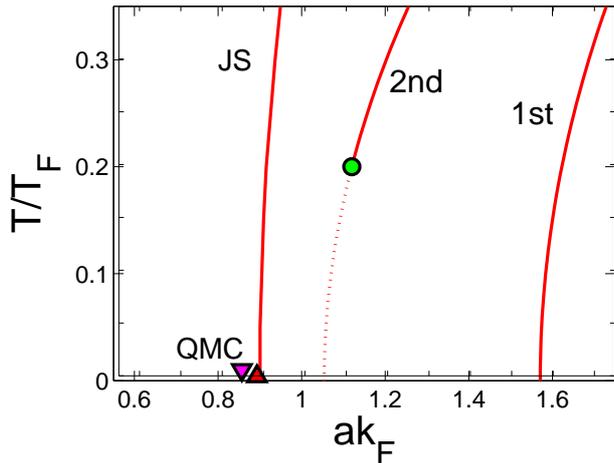
Figure 1: Phase diagram for a two-component Fermi gas with repulsive interactions. Full (dashed) curves indicate first (second) order PM to FM transitions within JS and dilute approximations with [6] and without [4] fluctuations. The circle indicates a tri-critical point. Triangles show the QMC transition points at zero temperature of Refs. [7, 8].

$f_T = -(\pi^2/4)(m^*/m)\sum_\sigma \rho_\sigma T^2/E_{F,\sigma}$ at low temperatures $T \ll E_{F,\sigma}$. In the dilute limit the effective mass $m^*/m = 1 + [8(7\ln 2 - 1)/15\pi^2]a^2 k_F^2$ in two-component symmetric systems only deviates from the bare mass to second order in the interaction parameter ak_F.

The density of the components are equal only in the PM phase and when the components are balanced initially. In the following we define an average Fermi wave number k_F from the total density $\rho = \nu k_F^3/6\pi^2$.

We postpone multicomponent systems to sec. VI and concentrate first on two spin states, e.g. $\sigma = \uparrow, \downarrow$ with total density $\rho = \rho_\downarrow + \rho_\uparrow$. The population of spin states are allowed to change (polarize) in order to observe phase transitions to itinerant ferromagnetism. The polarization (or magnetization) $P = (\rho_\downarrow - \rho_\uparrow)/\rho$ of the ground state phase is found by minimizing the free energy at zero magnetic field. The free energy of a low temperature ideal gas is $f_0 = E_F\rho(3/5 - \pi^2 T^2/4E_F^2)$. Expanding Eq. (1) for small polarization leads to a Ginzburg-Landau type equation for the free energy

$$\frac{f}{f_0} = 1 + \frac{10}{9\pi}ak_F + \frac{5}{9}\left[\frac{\chi_0}{\chi_T}P^2 + \frac{1}{27}P^4\right], \qquad (2)$$

to leading orders in interaction, polarization and temperature. Here $\chi_T = (\partial^2 f/\partial P^2)^{-1}$ is the isothermal spin-susceptibility given by

$$\frac{\chi_0}{\chi_T} = 1 - \frac{2}{\pi}ak_F + \frac{\pi^2}{12}\frac{T^2}{T_F^2}, \qquad (3)$$

where $\chi_0 = 3\rho/2E_F$ is the spin-susceptibility for an ideal gas at zero temperature. χ_T becomes singular when

$$ak_F = \frac{\pi}{2}\left(1 + \frac{\pi^2}{12}\frac{T^2}{T_F^2}\right), \qquad (4)$$

where the free energy of Eq. (2) predicts a second order phase transition from a PM to a FM (see Fig. 1) in accordance with the zero temperature result of Stoner [4]. The polarization is $P = \pm\sqrt{27(ak_F/\pi - 1/2)}$ at zero temperature but quickly leads to a locally fully polarized system $P = \pm 1$ due to the small fourth order coefficient in Eq. (2).

However, the predicted transition occurs close to the unitarity limit where the dilute equation of state Eq. (1) is not valid. Higher orders are important as exemplified by including fluctuations, i.e. the next order a^2 correction. As found in Refs. [5, 6] fluctuations change the transition from second to first order at low temperatures up to a tri-critical point at temperature $\simeq 0.2T_F$, where the transition becomes second order again (see Fig. 1). However, the 2nd order expansion is not valid either in the unitarity limit.

B. Jastrow-Slater approximation

The JS approximation applies to both strongly attractive and repulsive crossovers where it already has proven to be quite accurate for predicting universal functions and parameters. The JS approximation is the lowest order in a constrained variational (LOCV) approach to calculate the ground state energies of strongly correlated systems. It was developed for strongly interacting and correlated Bose and Fermi fluids respectively such as ^{4}He, ^{3}He and nuclear matter [11]. JS was among the earliest models applied to the unitarity limit and crossover of ultracold Fermi [12] and Bose [13] atomic gases. As explained in [11–13] the JS wave function

$$\Psi_{JS}(\mathbf{r}_1, ..., \mathbf{r}_N) = \Phi_S \prod_{i,j'} \phi(\mathbf{r}_i - \mathbf{r}_{j'}), \qquad (5)$$

incorporates essential two-body correlations in the Jastrow function $\phi(r)$. The Slater wave function Φ_S is a product of antisymmetrized free fermion wave functions for each spin. Each of these are the product of extended state free waves ($e^{i\mathbf{k_j}\cdot\mathbf{r}}$ with $|k_j| \leq k_F$) antisymmetrized to insure that same spins are spatially antisymmetric. The Jastrow wave function $\phi(r)$ only applies to particles with different spins (indicated by the primes). For attractive interactions it correlates different spins whereas for repulsive interactions it anti-correlates. The pair correlation function can be determined variationally by minimizing the expectation value of the energy, $E/N = \langle \Psi|H|\Psi \rangle / \langle \Psi|\Psi \rangle$, which may be calculated by Monte Carlo methods [8, 14]. At distances shorter than the interparticle spacing two-body clusters dominate and the Jastrow wave function $\phi(r)$ obeys the Schrödinger equation for a pair of particles of different spins interacting through a potential $U(r)$

$$\left[-\frac{\hbar^2}{m}\frac{d^2}{dr^2} + U(r)\right]r\phi(r) = 2\lambda r\phi(r), \qquad (6)$$

where the eigenvalue is the interaction energy of one atom $\lambda = E_{int}/N$. Most importantly, the boundary condition at short distances ($r = 0$) is given by the scattering length

$$\frac{(r\phi)'}{r\phi} = -\frac{1}{a}. \qquad (7)$$

Many-body effects become important when r is comparable to the interparticle distance $\sim k_F^{-1}$, but are found to be small [11–13]. Here the boundary conditions that $\phi(r > d_\sigma)$ is constant and $\phi'(r = d_\sigma) = 0$ are imposed at the healing distance d_σ, which is determined self consistently from number conservation

$$(\rho - \rho_\sigma) \int_0^{d_\sigma} \frac{\phi^2(r)}{\phi^2(d_\sigma)} 4\pi r^2 dr = 1. \qquad (8)$$

The prefactor $\rho - \rho_\sigma = \rho_{\sigma'}$ takes into account that a given spin σ only interacts and correlates with unlike spins $\sigma' \neq \sigma$. In the dilute limit $\phi(r) \simeq 1$ and so $d_\sigma = (9\pi/2)^{1/3} k_{F,\sigma'}^{-1}$. In the unitary limit $a \to \pm\infty$ the healing length approaches $d_\sigma = (3\pi)^{1/3} k_{F,\sigma'}^{-1}$ in stead. Generally the healing length is of order the Fermi wavelength of the other component, $d_\sigma k_{F,\sigma'} \sim 1$.

For a positive scattering length the interaction energy λ is positive and the solution to Eq. (6) is $r\phi(r) \propto \sin[k(r - b)]$ with $\lambda_\sigma = \hbar^2 k^2/2m$. Defining $\kappa_\sigma = k d_\sigma$ the boundary conditions and number conservation requires [13]

$$\frac{a}{d_\sigma} = \frac{\kappa_\sigma^{-1} \tan \kappa_\sigma - 1}{1 + \kappa_\sigma \tan \kappa_\sigma}. \qquad (9)$$

The resulting interaction energy reproduces the correct dilute limit result of Eq. (1). In the unitarity limit $a \to +\infty$, the positive energy solution reduces to $\kappa \tan \kappa = -1$ with multiple solutions $\kappa_1 = 2.798..$, $\kappa_2 = 6.121..$, etc., and asymptotically $\kappa_n = n\pi$ for integer n. In addition there is one negative energy solution for $n = 0$ with $\kappa_0 = 1.997..$ which corresponds to the BCS-BEC crossover when $a \to -\infty$. Generally, $n = 0, 1, 2, ..$ is the number of nodes in the Jastrow wave function and each determines a new universal limit with universal parameters depending on the number of nodes. The phase in the wave function is $kb = \pi(n - 1/2)$ whenever the unitary limit of n nodes is encountered.

It should be emphasised that for positive scattering lengths the wave function and thus the correlations function between fermions of unlike spin and bosons $\propto r\phi \sim \sin(kr - b)$ has a node at b/k which is somewhere within the interparticle distance. It does not vanish as $r \to 0$ as does the wave function for a short range repulsive potential as in hard sphere scattering where $a \simeq R$. Therefore the Gutzwiller approximation may well apply for hard sphere gases, strongly correlated nuclear fluids and liquid helium as discussed in [10] but it does not apply to the repulsive unitarity limit of ultracold gases when the wave function has to obey the short range boundary condition of Eq. (7).
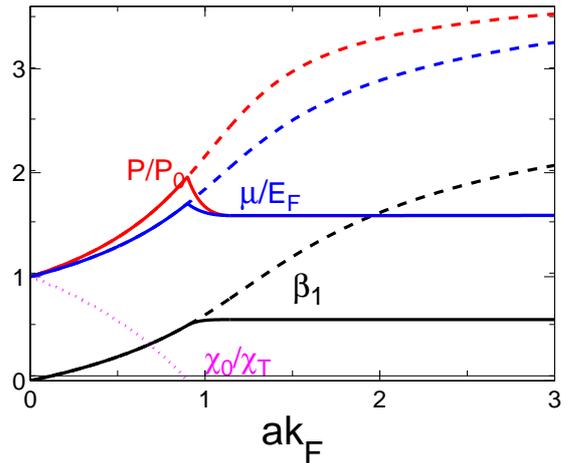

Figure 2: (Color online) Universal functions calculated within JS at zero temperature vs. repulsive interaction: the ratio of interaction and kinetic energy β, the pressure and chemical potential and the inverse spin susceptibility χ_0/χ_T, all with respect to their non-interactive values. Note that χ_T diverges at $ak_F = 0.90$ due to the FM instability. Full curves include the FM transition whereas the dashed have FM suppressed, i.e. remain in the PM phase.

It is customary to define the universal function $\beta = E_{int}/E_{kin}$ as the ratio of the interaction E_{int} and kinetic energy $E_{kin} = (3/5)E_F$. In the JS model the interaction energy per particle is $E_{int} = \hbar^2 k^2/2m = \kappa^2/2md^2$ and thus $\beta = (5/3)\kappa^2/k_F^2 d^2$ in the PM phase. In the FM phase the spin densities differ and the ratio of the average interaction to kinetic energy can be considerably lower than β as shown in Fig. (2).

Because Eq. (9) has a string of solutions for a given scattering length or $k_F a$, κ and β are multivalued functions which we distinguish by the index $n = 0, 1, 2, ...$ referring to the number of nodes in the many-body wave function between any two atoms [12]. β_0 has been studied extensively in the BCS-BEC crossover and β_1 in the repulsive crossover [1–3]. In the repulsive unitarity limit $n = 1$ the universal parameter is $\beta_1(k_F a \to \infty) = 5\kappa_1^2/3(3\pi)^{2/3} \simeq 2.93$. It has recently been measured for a ^{6}Li gas in two spin states [1]. The chemical potential in the optical trap almost doubles going from the non-interacting to the unitarity limit. Since it scales as $\mu \propto \sqrt{1 + \beta_1(\infty)}$ we obtain $\beta_1(\infty) \sim 3$ compatible with JS. In the following we concentrate on repulsive interactions and use $\beta = \beta_1$.

The interaction energy for an atom with spin σ depends on the density of unlike spins and is given by $\lambda = \kappa_\sigma^2/2md_\sigma^2 \equiv (3/5)E_{F\sigma'}\beta(ak_{F,\sigma'})$, where β is the universal function for repulsive interactions. We obtain the total energy density at zero temperature by adding the Fermi kinetic energy and the interaction energy λ_σ, and
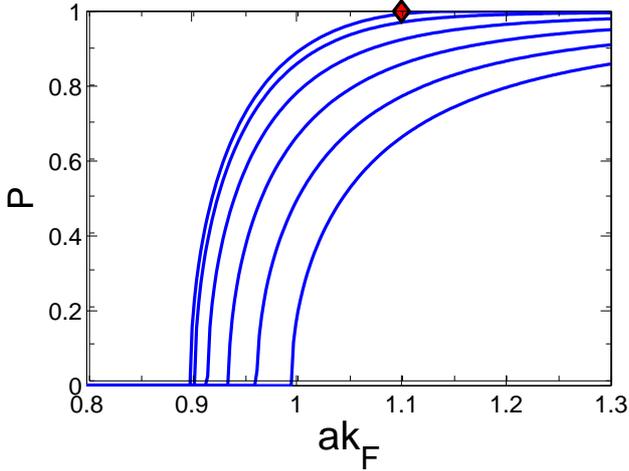
Figure 3: (Color online) Polarization vs. ak_F at $T/T_F = 0, 0.1, 0.2, ..., 0.5$ from left to right. The second order transition yields a steep but continuous transitions $P \propto \sqrt{ak_F - ak_c}$. The diamond indicates the transition point to a pure one-component ($P = \pm 1$) FM at zero temperature.

Figure 4: (Color online) Compressibility and polytropic index vs. repulsive scattering length (ak_F^0) at zero temperature. Both are second derivates of the free energy and are therefore discontinuous at the FM transition.

sum over particle densities [11, 12]

$$f = \frac{3}{5} \sum_{\sigma} E_{F,\sigma} \rho_\sigma + \frac{3}{5} \sum_{\sigma \neq \sigma'} E_{F,\sigma'} \beta(ak_{F,\sigma'}) \rho_\sigma + f_T \quad (10)$$

including a thermal free energy f_T as given above. This expression generalizes the standard expression for the energy density $E/V = (3/5)E_F(1 + \beta)\rho$ to finite polarization and temperature. The result can be understood from dimensional arguments as β is dimensionless and gives the repulsive energy of particles of spin σ due interactions with particles of opposite spin. Note that the interaction energy and its dependence on polarization is given in terms of one universal function β of one variable only. As shown in Fig. 2 the ratio of the interaction to kinetic energy is reduced by the FM transition w.r.t β.

Expanding Eq. (10) for small polarization gives

$$\frac{f}{f_0} = 1 + \beta + \frac{5}{9} \frac{\chi_0}{\chi_T} P^2 + \mathcal{O}(P^4), \quad (11)$$

where the isothermal spin susceptibility is

$$\frac{\chi_0}{\chi_T} = 1 - \frac{7}{5}\beta - \frac{2}{5}ak_F\beta' + \frac{1}{10}(ak_F)^2\beta'' + \frac{\pi^2}{12}\frac{T^2}{T_F^2}, \quad (12)$$

with $\beta' = d\beta/d(ak_F)$ and $\beta'' = d^2\beta/d(ak_F)^2$. In the dilute limit $\beta = (10/9\pi)ak_F$ and Eqs. (11) and (12) reduce to Eqs. (2) and (3) respectively.

The spin-susceptibility calculated within JS is shown in Fig. 2 at zero temperature. It diverges at $ak_F \simeq 0.90$ where the universal function is $\beta_{FM} \simeq 0.53$. By equating the energy of the unpolarized gas, $\sim (1 + \beta)$ with that of a fully polarized (one-component) gas, $\sim 2^{2/3}$, we find that a first order transition requires $\beta = 2^{2/3} - 1 \simeq$
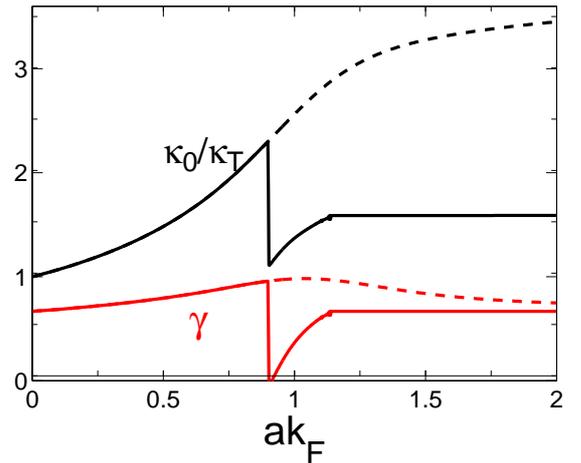
$0.59 > \beta_{FM}$, and therefore JS predicts a second order FM transition as shown in Fig. 1. This transition point is in remarkable agreement with two recent QMC calculations which find $ak_F = 0.86$ [7] and $ak_F = 0.89$ [8]. The QMC calculations could not determine the order of the transition within numerical accuracy. In the BCS-BEC crossover a minor discrepancy was found between JS [12] and QMC [14, 15] which partly could be attributed to pairing which is excluded in the JS wave function but included in the QMC calculations with attractive interactions. Since pairing is absent for repulsive interactions in both QMC and the JS model, they are expected to match better near the FM transition. Note that the JS wave function is also used as a starting point in the QMC calculations of Refs. [8, 14, 15].

Minimizing the free energy of Eq. (11) we obtain the polarization $P \propto \sqrt{-\chi_0/\chi_T}$ at the onset of FM as shown in Fig. 3 at low temperatures. Full polarization is reached at $ak_F \simeq 1.1$ at zero temperature only.

The spin-susceptibility is related to the spin-antisymmetric Landau parameter as $F_0^A = (m^*/m)\chi_0/\chi_T - 1$. The effective mass $m^* = m$ is implicitly assumed in the JS energy of Eq. (10). It has recently been measured in the BCS-BEC unitarity limit $m_0^*/m = 1.13 \pm 0.03$ [16] but not for the repulsive crossover yet. Since β at the FM transition point is comparable to $|\beta_0|$, these two effective masses may be expected to be similar. The small deviation from $m^* = m$ only changes the universal functions and the phase diagram slightly at higher temperature. The order and the position of the transition is unchanged at zero temperature.

III. NUMBER FLUCTUATIONS

The density or local number fluctuations have recently been measured in shot noise experiments for an ideal ultracold Fermi gas and by speckle noise in the BCS-BEC crossover [17, 18]. The number fluctuations are measured in a small subvolume of the atomic cloud with almost uniform density. The fluctuations in spin and total number of atoms are directly related to the spin susceptibility and compressibility respectively.

The local fluctuations in total number can for a large number of atoms be related to the isothermal compressibility $\kappa_T = \rho^{-2}(\partial\rho/\partial\mu)_{V,T}$, by the fluctuation-dissipation theorem

$$\frac{(\Delta N)^2}{N} = \frac{3}{2}\frac{T}{T_F}\frac{\kappa_T}{\kappa_0}\,. \qquad (13)$$

Here, $\kappa_0 = 3/(2\rho E_F)$ is the compressibility for an ideal Fermi gas at zero temperatures. An ideal classical gas has $\kappa_T = 1/(\rho k_B T)$ such that the number fluctuations are Poisson: $(\Delta N)^2/N = 1$. The compressibility is related to the symmetric Landau parameter as $F_0^S = (m^*/m)\kappa_0/\kappa_T - 1$.

The compressibility can generally be expressed in terms of the universal function β [20] at zero temperature

$$\frac{\kappa_0}{\kappa_T} = 1 + \beta + \frac{4}{5}ak_F\beta' + \frac{1}{10}(ak_F)^2\beta'', \qquad (14)$$

in the PM phase. Once the FM transition sets in, the ground state energy of Eq. (10) is lowered due to finite polarization and the inverse compressibility drops as shown in Fig. 4 for JS. It is discontinuous when the second order FM transition sets in because it is a second derivative of the free energy which is softened by the spin-susceptibility term in Eq. (11). In the pure one-component FM phase the compressibility is that of an ideal one-component gas $\kappa_0/\kappa_T = 2^{2/3}$. The peculiar and discontinuous behaviour of the compressibility at the FM transition is directly reflected in the fluctuations in total number according to Eq. (13).

If the FM transition was first order the compressibility diverges at the phase transition, i.e., κ_0/κ_T vanishes in part of the density region where $0 < P < 1$ (see Figs. 3+4). Consequently, the number fluctuation also diverges according to Eq. (13) reflecting the density discontinuity at a first order transition.

The fluctuation-dissipation theorem also relates the thermal spin fluctuations to the spin susceptibility

$$\frac{\Delta(N_\uparrow - N_\downarrow)^2}{N} = \frac{3}{2}\frac{T}{T_F}\frac{\chi_T}{\chi_0}\,. \qquad (15)$$

At the FM instability the spin-susceptibility and therefore also the spin fluctuations diverge reflecting that phase separation occurs between domains of polarization $\pm P$. Such domains were, however, not observed in the experiments of [1] within the spatial resolution of the experiment.

IV. TRAP RADII AND KINETIC ENERGIES

In experiments the atoms are confined in harmonic traps. For a sufficiently large number $N = \sum_\sigma N_\sigma$ of particles confined in a (shallow) trap the system size R_σ is so long that density variations and the extent of possible phase transition interfaces can be ignored and one can apply the local density approximation. The total chemical potential is given by the sum of the harmonic trap potential and the local chemical potential $\mu_\sigma = (df/d\rho_\sigma)_{V,T}$

$$\mu_\sigma(r) + \frac{1}{2}m\omega^2 r^2 = \frac{1}{2}m\omega^2 R_\sigma^2\,, \qquad (16)$$

which must be constant over the lattice for all components $\sigma = 1, 2, .., \nu$. It can therefore be set to its value at its edge R_σ, which gives the r.h.s. in Eq. (16). The equation of state determines the chemical potentials μ_σ in terms of the universal function of Eq. (10).

In a two-component spin-balanced system the chemical potential and radii of the two components are equal (denoted μ and R in the following). In the FM phase their densities $\rho(1 \pm P)$ differ but these FM spin domains coexist. Using the JS EoS of Eq. (10) to calculate the chemical potential we can find the density distribution from chemical equilibrium Eq. (16) including phase transitions and calculate cloud radii R, the root mean square $RMS = \sqrt{\langle r^2\rangle}$ and kinetic energy $E_{kin} = \langle k_F^2/2m\rangle$ averaged over all particles in the trap. These are shown in Fig. 5 normalized to their values trapped non-interacting ultracold atoms, $R_0 = (24N)^{1/6}a_0$, $RMS_0 = \sqrt{3/8}R_0$ and $E_{kin}^0 = (3/8)E_F^0$ respectively. Here, $E_F^0 = (\hbar k_F^0)^2/2m$ and $k_F^0 = (24N)^{1/6}/a_0$ are the Fermi energy and wave number in the centre of the trap for non-interacting atoms and $a_0 = \sqrt{\hbar/m\omega}$ is the oscillator length. Repulsive interactions reduce the central density and Fermi energy as can be seen from k_F/k_F^0 shown in Fig. 5. As a consequence the radii increase except for the RMS radius above the FM transition (see Fig. 5). It decreases because atoms are redistributed from the PM phase near the surface to the FM phase in the centre. The kinetic energy of the atoms has the opposite behaviour because repulsion increases the interaction energy in the PM phase at the cost of the kinetic energy.

In the recent experiment of Ref. [1] a transition is observed around $ak_F^0 \simeq 2.2$ at temperatures $T/E_F^0 = 0.12$ (and $ak_F^0 \simeq 4.2$ at $T/E_F = 0.22$), which is compatible with the first order calculation of Ref. [19]. This transition point is a factor of ~ 2 larger than the FM transition point calculated in all models [4–8] as well as JS. Rescaling ak_F^0 by a factor 2 we find very good quantitative and qualitative agreement with the data of [1] as was found in the second order calculation of Ref. [6]). The distinct transitions in the radii, kinetic energies and atomic losses are well reproduced qualitatively and quantitatively after rescaling ak_F^0 by a factor 2. It is currently not understood why all the higher order and QMC calculations lead to a larger discrepancy than the simpler first order when
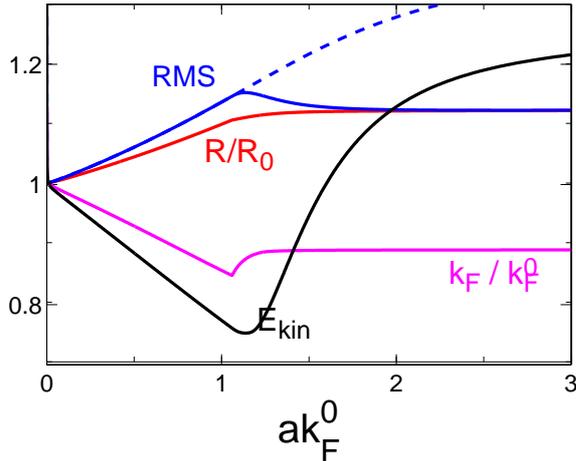
Figure 5: (Color online) Radius of the trapped cloud, RMS radius, kinetic energy and central Fermi wavenumber all at zero temperature and relative to their non-interaction values vs. repulsive scattering length (ak_F^0). Dashed curved shows the RMS radius for a PM phase where the FM transition is inhibited. Due to repulsion the central density and thus k_F is lower.

compared to experiments. As discussed above there are no pairing interaction in neither QMC nor the JS model for repulsive interactions. However, the strongly repulsive interaction limit is metastable w.r.t. three-body interactions as well as a transition to the paired BCS state with no nodes in the Jastrow two-body correlation function, and it could be responsible for the earlier on-set of the FM transition.

Another puzzling result was the apparent absence of FM domains within the spatial resolution of the experiment of Ref. [1]. We suggest to start out with an unbalanced spin system where macroscopic FM domain sizes can be realized and direct observation of large FM domains is possible. As the repulsion is increased the RMS radii of the minority spins increases faster than that of the majority spins. When the FM transition occurs the system favours a core with predominantly majority spins surrounded by a mantle of both spins in a PM phase. With increasing spin imbalance the majority spin purity of the FM core increases, i.e. the domains are effectively separated on a large scale. The amount of separation and change in radii will depend on the overall spin imbalance.

Three component systems with more than one Feshbach resonance as in ^{6}Li are also more complicated. For example, when the Feshbach magnetic field is such that two resonances a_{12} and a_{13} are large but a_{23} small, the atoms will separate between a FM phase of 1 and a mixed FM phase of 2+3 with different densities.

V. COLLECTIVE MODES

Collective modes have been studied intensively in the BCS-BEC crossover where they reveal important information of the equation of state (EoS) and determine $\beta_0(ak_F)$. When the EoS can be approximated by a simple polytrope $P \propto \rho^{\gamma+1}$ the collective eigen-frequencies can be calculated analytically [20, 21] in terms of the polytropic index γ. Even when the EoS is not a perfect polytrope the collective modes in the BCS-BEC crossover could be described well using the effective polytropic index at densities near the centre of the trap given by the logarithmic derivative [20]

$$\gamma \equiv \frac{\rho}{P}\frac{dP}{d\rho} - 1 = \frac{\frac{2}{3}(1+\beta) + \frac{5}{6}ak_F\beta' + \frac{1}{6}(ak_F)^2\beta''}{1 + \beta + ak_F\beta'/2} \quad (17)$$

We therefore calculate γ within JS for repulsive interactions as shown in Fig. 4. Like the compressibility it has a discontinuity at the FM phase transition because it is a second derivative of the free energy with a second order transition. In both the dilute limit and pure FM phase the gas is ideal with polytropic index $\gamma = 2/3$.

For a very elongated or cigar-shaped trap (prolate in nuclear terminology), $\lambda \ll 1$, used in most experiments [22, 23], the collective breathing modes separate into a low frequency axial mode with oscillation frequency $\omega_{ax} = \sqrt{3 - (\gamma+1)^{-1}}\,\omega_3$ and a radial mode with $\omega_{rad} = \sqrt{2(\gamma+1)}\,\omega_0$ [21].

The spin dipole mode is more complicated because it is sensitive to the spin susceptibility which diverges at the FM transition point. The EoS is far from polytropic and the delicate calculation of spin dipole modes with diverging spin susceptibility is beyond the scope of this work. The spin dipole mode is estimated within a sum rule approach in Ref. [24].

VI. MULTICOMPONENT SYSTEMS

Interesting information on the order of the FM transition can be obtained by generalizing the above results to Fermi gases with more that two spin states such as ^{6}Li with $\nu = 3$ hyperfine states [25], ^{137}Yb with six nuclear spin states [26], and heteronuclear mixtures of ^{40}K and ^{6}Li [27]. The interactions and phases can be very complicated when the Feshbach resonances between various components differ as for ^{6}Li. In the following we restrict ourselves to multi-components with the same relative scattering length a.

In the dilute case the condition for a first order phase transition in a ν component system can be found from the energy density of Eq. (1). The preferred transition is directly from $\nu = 1$ to a domains of one-components system $\nu = 1$ which occurs when

$$ak_F = \frac{9\pi}{10}\frac{\nu^{2/3}-1}{\nu-1}\left(1 + \frac{5\pi^2}{12}\frac{T^2}{T_F^2}\nu^{-2/3}\right). \quad (18)$$

At zero temperature this condition is $ak_F \simeq 1.66, 1.53, 1.43, 1.36$, etc. for $\nu = 2, 3, 4, 5, 6, ..$ respectively. The condition for a second order transition is found by expanding the dilute multi-component free energy for small polarization. One finds the same spin susceptibility as in the two-component case, Eq. (4), and therefore the putative the second order transition remains at $ak_F = \pi/2 \simeq 1.57$. Comparing numbers we conclude that at zero temperature the second order transition occurs for $\nu = 2$ only in the dilute case whereas for $\nu \geq 3$ the FM transition is first order and given by Eq. (18). At finite temperatures the second order transition of Eq. (3) match the first order of Eq. (18) at a temperature which determines the tri-critical point (ak_F, T) in the phase diagram for $\nu \geq 3$ as shown in Fig. 6.

The free energy of the JS model, Eq. (10), also applies to multi-component systems. The condition for a first order FM transition to coexisting fully polarized (one-component) FM domains is

$$\beta(ak_F) = \frac{\nu^{2/3} - 1}{\nu - 1}\left(1 + \frac{5\pi^2}{12}\frac{T^2}{T_F^2}\frac{m^*}{m}\nu^{-2/3}\right). \quad (19)$$

At zero temperature the FM transition occurs for $\beta = 0.59, 0.54, 0.51, 0.48, ..$ at $ak_F = 0.96, 0.91, 0.87, 0.84, ..$ for $\nu = 2, 3, 4, 5, ..$ respectively. As in the dilute case the spin-susceptibility is unchanged, Eq. (12), in the JS model and the putative second order transition remains when $\beta = 0.53$ at $ak_F = 0.90$. Thus the FM transition at is at zero temperature marginally second order for $\nu \leq 3$ but first order for $\nu \geq 4$. Again the tri-critical points (ak_F, T) are determined by the matching condition for the first Eq. (19) and second Eq. (12) order transitions and are shown in Fig. 6.

Generally the difference between first and second order FM transition is small which may explain why QMC could not determine the order within numerical accuracy [7, 8]. First order transitions to partially polarized FM does not occur for two-component systems but may be possible in multi-component systems.

The marginal first vs. second order FM transition for $\nu = 3$ is analogous to the marginal stability in the unitary limit of the BCS-BEC crossover [12]. Here it is known that two-component systems are stable but four-component systems are unstable as in nuclear matter.

VII. SUMMARY AND OUTLOOK

By extending the Jastrow-Slater approximation to finite polarization and temperature we have calculated a number of thermodynamic functions and observables for cold Fermi atoms with repulsive interactions. In particular we found a second order FM phase transition at $ak_F \simeq 0.90$ at zero temperature in close agreement with

QMC. The compressibility and spin susceptibility were calculated and the resulting observables like the fluctuations in total number and spin as well as collective modes
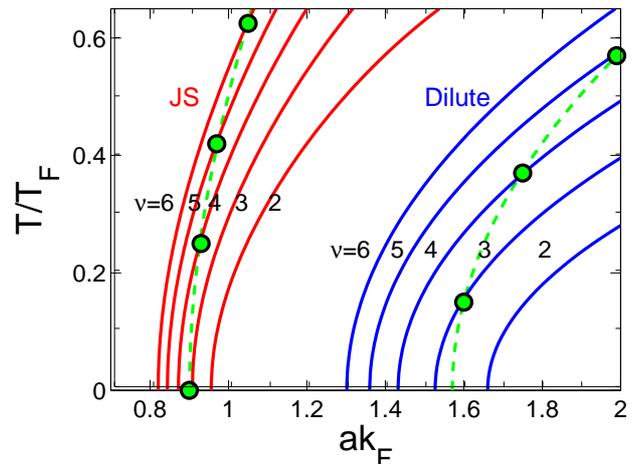

Figure 6: (Color online) Phase diagrams for multi-component ($\nu = 2, 3, 4, 5, 6$ from left to right) Fermi gases with repulsive interactions. Full (dashed) curves indicate first (second) order PM to FM transitions within JS and dilute approximations. Circles indicate the tri-critical points where the transition changes from first to second order at higher temperatures.

are discontinuous at the transition point. These can be distinguished from a first order transition where, e.g., the compressibility diverges.

For trapped gases the radii and kinetic energies also have characteristic behaviour as function of repulsive interaction strength when the FM transition occurs in the centre. If the interaction strength is reduced by a factor ~ 2 the radii and kinetic energies of JS and Ref. [6] agree qualitatively and quantitatively with experiments [1]. In order to observe the FM domains we suggest to start out with a spin-imbalanced system of two-component Fermi atoms and tune the magnetic field towards the Feshbach resonance from the repulse side where the FM transition sets in. As result the core will be a large domain of the majority spin only which exceeds the experimental domain size resolution.

It would be interesting to study multi-component systems such as the three component ^{6}Li system near Feshbach resonances where bulk separation between the spin component domains is predicted to take place. Multi-component systems with the same interactions (and scattering lengths) between states display interesting phase diagrams with first to second order tri-critical points when the number of components exceeds two in the dilute case and three in the JS model.

References

[1] G-B. Jo et al., Science **325**, 1521-1524 (2009); see also comment ArXiv:0910.3419.

[2] T. Bourdel et al., Phys. Rev. Lett. **91**, 020402 (2003); cond-mat/0403091; J. Cubizolles et al., cond-mat/0308018

[3] S. Gupta et al., Science **300**, 47 (2003).

[4] E. Stoner, *Phil. Mag.* **15**, 1018 (1933).

[5] R. A. Duine & A. H. MacDonald, Phys. Rev. Lett. **95**, 230403 (2005).

[6] G. J. Conduit, B. D. Simons, arXiv:0907.3725.

[7] S. Pilati, G. Bertaina, S. Giorgini, M. Troyer, arXiv/1004.1169

[8] S.-Y. Chang, M. Randeria, N. Trivedi, arXiv.org/1004.2680

[9] G. J. Conduit, B. D. Simons, Phys. Rev. Lett. **103**, 200403 (2009).

[10] H. Zhai, Phys Rev. A **80**, 051605(R) (2009).

[11] V. R. Pandharipande, Nucl. Phys. A **174**, 641 (1971) and **178**, 123 (1971); Pandharipande, V. R., and Bethe, H. A., Phys. Rev. C **7**, 1312 (1973);

[12] H. Heiselberg, Phys. Rev. A **63**, 043606 (2001); J. Phys. B: At. Mol. Opt. Phys. **37**, 1 (2004).

[13] S. Cowell, H. Heiselberg, I. E. Mazets, J. Morales, V. R. Pandharipande, and C. J. Pethick, Phys. Rev. Lett. **88**, 210403 (2002). J. Carlson, H. Heiselberg, V. R. Pandharipande, Phys. Rev. C **63**, 017603 (2000).

[14] G.E. Astrakharchik, J. Boronat, J. Casulleras, S. Giorgini, Phys. Rev. Lett. **93**, 200404 (2004).

[15] J. Carlson, S-Y. Chang, V. R. Pandharipande, K. E. Schmidt, Phys. Rev. Lett. **91**, 50401 (2003); S-Y. Chang, V.R. Pandharipande, J. Carlson, K. E. Schmidt, Phys. Rev. A **70**, 043602, 2004; Nucl. Phys. A **746**, 215, 2004.

[16] S. Nascimbene, N. Navon, K.J. Jiang, F. Cevy, C. Salomon, Nature 463 (2010) 1057

[17] C. Sanner, E. J. Su, A. Keshet, R. Gommers, Y. I. Shin, W. Huang, W. Ketterle, Phys. Rev. Lett. 105, 040402 (2010); arXiv:1010.1874

[18] T. Müller, B. Zimmermann, J. Meineke, J. Brantut, T. Esslinger, H. Moritz, arXiv:1005.0302

[19] L. J. LeBlanc, J. H. Thywissen, A. A. Burkov, A. paramekanti, arXiv:0903.5343

[20] H. Heiselberg, Phys. Rev. Lett. **93**, 040402 (2004).

[21] M. Cozzini, S. Stringari, Phys. Rev. A **67**, 041602 (R) (2003).

[22] K. M. O'Hara, S. L. Hemmer, M. E. Gehm, S. R. Granade, J. E. Thomas, Science **298** (2002) 2179. L. Luo, B. Clancy, J. Joseph, J. Kinast, J. E. Thomas Phys. Rev. Lett. **98**, 080402 (2007).

[23] M. Bartenstein, A. Altmeyer, S. Riedl, S. Jochim, C. Chin, J. HeckerDenschlag, R. Grimm, Phys. Rev. Lett. **92**, 203201 (2004)

[24] A. Recati and S. Stringari, arXiv:1007.4504.

[25] S. Jochim et al., Phys. Rev. Lett. **91**, 240402 (2003); M. Bartenstein et al., ibid. **92**, 120401 (2004). T. B. Ottenstein, T. Lompe, M. Kohnen, A. N. Wenz, S. Jochim, Phys. Rev. Lett **101**, 203202 (2008).

[26] M. Kitagawa et al., Phys. Rev. A **77**, 012719 (2008).

[27] F. M. Spiegelhalder et al., arXiv:0908.1101; E. Wille et al., Phys. Rev. Lett. **100**, 053201 (2008)